

See discussions, stats, and author profiles for this publication at: <https://www.researchgate.net/publication/231375997>

Absorption and Oxidation of Nitric Oxide (NO) by Aqueous Solutions of Sodium Persulfate in a Bubble Column Reactor

ARTICLE *in* INDUSTRIAL & ENGINEERING CHEMISTRY RESEARCH · AUGUST 2010

Impact Factor: 2.59 · DOI: 10.1021/ie100607u

CITATIONS

35

READS

157

2 AUTHORS:



[Nymul Khan](#)

Pennsylvania State University

8 PUBLICATIONS 58 CITATIONS

[SEE PROFILE](#)



[Yusuf Adewuyi](#)

North Carolina Agricultural and Technical ...

52 PUBLICATIONS 1,663 CITATIONS

[SEE PROFILE](#)

Absorption and Oxidation of Nitric Oxide (NO) by Aqueous Solutions of Sodium Persulfate in a Bubble Column Reactor

Nymul E. Khan and Yusuf G. Adewuyi*

Department of Chemical and Bioengineering, North Carolina A&T State University,
Greensboro, North Carolina 27411

The absorption–oxidation of nitric oxide (NO) by aqueous solution of sodium persulfate ($\text{Na}_2\text{S}_2\text{O}_8$) has been studied in a bubble column reactor operated in semibatch mode. The effects of different process variables such as the persulfate concentration (0.01–0.2 M), temperature (23–90 °C), pH (4–12), sodium chloride concentration (0–0.5 M), and NO concentration (500–1000 ppm) were studied. In general, the NO fractional conversion (percent of inlet NO removed) at all temperatures increased almost linearly with persulfate concentration up to about 0.1 M, after which it started to level off. Increased temperature led to an increased fractional conversion of NO at all persulfate levels. At 0.1 M persulfate concentration, conversions of up to 69% and 92% were observed at 70 and 90 °C, respectively. Solution pH and chloride concentration were both found to affect NO absorption at higher temperatures. The effect of pH was moderate, but sodium chloride showed a significant effect on NO absorption at 70 °C, to the point of causing complete removal of NO. The effect of initial NO concentration in the gas phase was found to be marginal. The results demonstrate the feasibility of NO removal using aqueous solutions of sodium persulfate.

Introduction

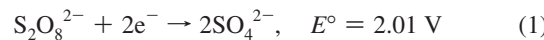
NO_x (nitric oxide and its group of compounds) and SO_2 released from coal-fired power plants cause considerable environmental and health problems. NO_x is one of the main ingredients involved in the formation of ground-level ozone, urban smog, and acid rain, as well as in the occurrence of eutrophication and respiratory and heart diseases. Since the adoption of the Clean Air Act in 1970, whereas the levels of many air pollutants such as NO_2 and SO_2 have decreased, the level of NO has actually increased by 20%.¹ Thus, stricter control by state and regulatory agencies for NO_x emissions justifies the need for efficient and inexpensive NO_x removal technologies that can be easily retrofitted to existing power plants. Currently, popular technologies for NO_x abatement include selective catalytic reduction (SCR), selective noncatalytic reduction (SNCR), flue gas recirculation (FGR), and thermal treatments. All of these technologies suffer from some form of drawbacks including high operating and capital costs, high temperatures, and disposal problems. In this respect, NO_x removal by aqueous scrubbing promises to be an inexpensive and efficient technology. However, whereas SO_2 and NO_2 are quite easily removed by wet scrubbing mechanisms, NO is much more difficult to remove because it is very sparingly soluble in aqueous solutions, which greatly increases the liquid-phase resistance to mass transfer.^{2,3}

Numerous chemical oxidants have been studied for their effectiveness in NO_x removal by wet scrubbing. The various chemicals that have been studied include water-soluble ferrous-chelating agents, hydrogen peroxide (H_2O_2) and peracids, yellow phosphorus, organic hydroperoxides, sodium chlorite (NaClO_2), potassium permanganate (KMnO_4), sodium hypochlorite, and peroxyomonosulfate (oxone).^{2,3} We previously reported the absorption and oxidation of NO_x in aqueous solutions of peroxyomonosulfate or oxone (with the active ingredient HSO_5^-) in a bubble column reactor using NO feed concentrations of about 500 and 1000 ppm.³ It was shown that (1) the fractional

removal ranged from 60% to 86%, (2) the highest removal of NO occurred at the lowest gas flow rate of 0.1 standard liters per minute (SLPM) for the range of flow rates tested (0.1–1.0 SLPM), (3) the NO removal efficiency was not significantly affected by temperature in the range of 22–55 °C, (4) the presence of SO_2 increased the overall fractional conversion of NO, and (5) the optimal fractional conversion occurred with 0.02 M oxone in the pH range of 6.5–8.5. The rate of reaction was found to be first-order with respect to NO and zeroth-order with respect to HSO_5^- . Our results demonstrated the feasibility of removing NO_x and SO_x simultaneously by low-temperature aqueous scrubbing using oxone.

Despite the various research efforts, the industrial use of wet scrubbing for NO_x removal has been discouraged because of the added costs of chemicals and disposal of the spent solution. Therefore, an inexpensive, efficient, and environmentally benign chemical needs to be found. Sodium persulfate could be one such compound. It is a strong oxidant, has an excellent shelf life when stored properly, and is very inexpensive. It satisfies many of the criteria for being a candidate for the chemical oxidant used in the wet scrubbing of NO_x and it has previously been used in wet scrubber for the treatment of toxic gases [namely, benzene, toluene, ethylbenzene, and xylenes (BTEX)].^{4,5} Also, in the presence of impurities in the aqueous phase, such as bicarbonates, persulfate is far more chemically stable than hydrogen peroxide, which is a more widely used oxidant.⁶ This makes persulfate an even more attractive oxidant.

The persulfate ion is one of the strongest oxidizing agents in aqueous solutions. The standard oxidation–reduction potential (E°) for the half-cell persulfate reaction is 2.01 V, comparable to those of ozone and hydrogen peroxide, both of which are widely used in wastewater treatment.^{3,7–10}



Although persulfate anion is a strong oxidizing agent, it is kinetically slow under ordinary conditions.⁸ Persulfate can be activated by heat, light, or metal catalysts. It is well-known that,

* To whom correspondence should be addressed. E-mail: adewuyi@ncat.edu.

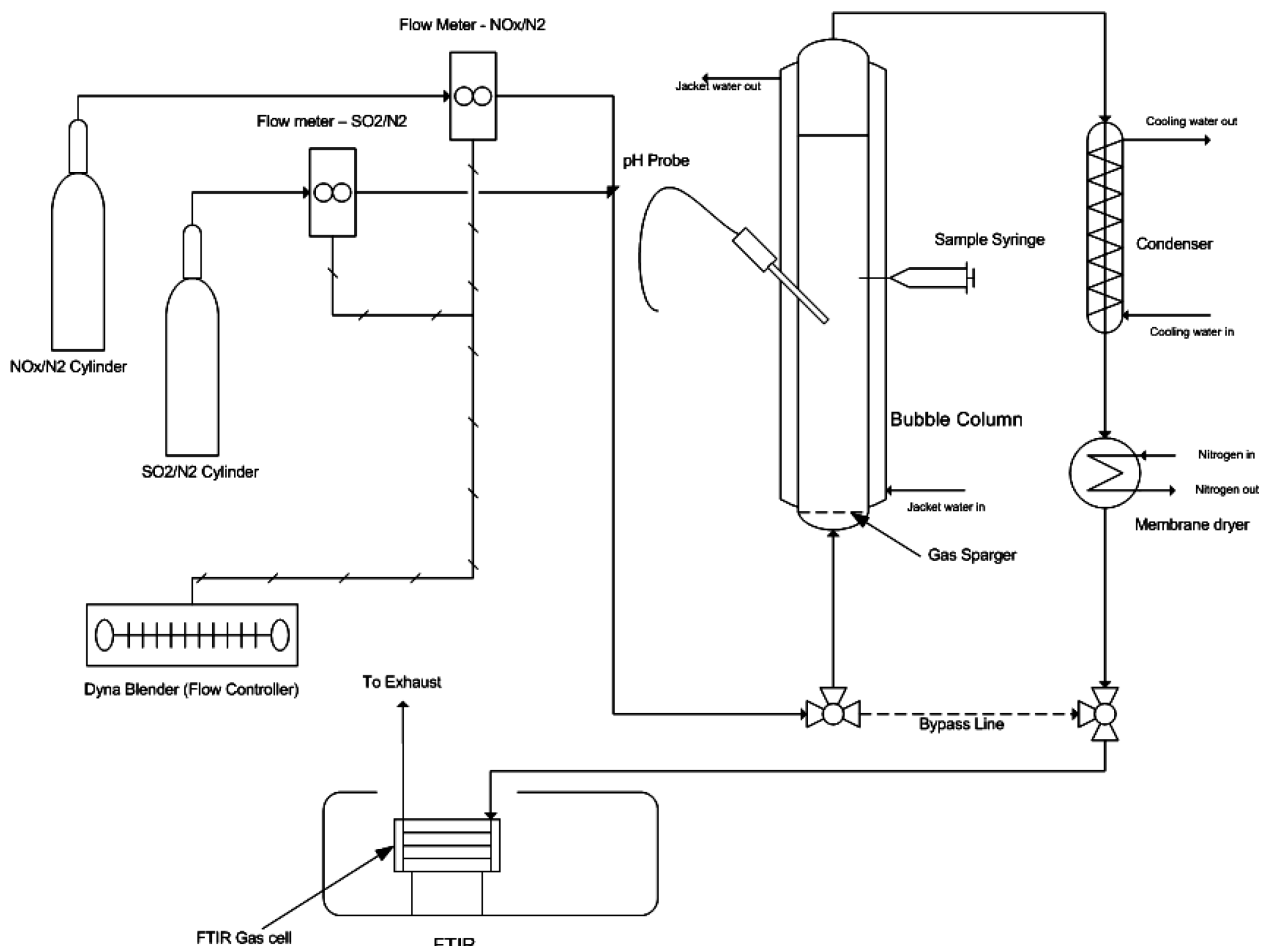
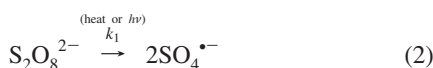


Figure 1. Schematic diagram of the experimental setup.

when activated, persulfate generates the intermediate sulfate free radical ($\text{SO}_4^{\cdot-}$)^{11,12}



Activated persulfate has found use in various applications including olefin polymerization,¹³ environmental remediation of organic contaminants,¹⁴ and measurement of total organic carbon (TOC).¹⁵ Because of its stability before being activated, the use of persulfate is also becoming increasingly popular in the in situ chemical oxidation (ISCO) of groundwater contamination.¹⁶ This involves activating persulfate directly at a contaminated source zone in order to oxidize contaminants into harmless end products within the soil matrix. These developments prompted us to investigate the potential for the use of sodium persulfate in the aqueous scrubbing of NO_x .

In this work, the feasibility of utilizing sodium persulfate to absorb and oxidize NO was determined using a bubble column reactor. The effects of different process variables, such as temperature, persulfate concentration, solution pH, and the presence of sodium chloride (prevalent in flue gas scrubbing systems and one of the sources of solution ionic strength), on the fractional conversion of NO were determined. In addition, a simple model was developed to correlate the experimental data.

Experimental Details

Reagents. The chemicals used in the experiments were sodium persulfate ($\text{Na}_2\text{S}_2\text{O}_8$, powder, >98%; Acros Organics,

Morris Plains, NJ), phosphate buffer (mixture of NaOH and KHPO_4 , $\text{pH} = 7.0 \pm 0.02$ at 25°C ; Fisher Scientific, Pittsburgh, PA) and sodium hydroxide (pellets, >97%, ACS reagent; Aldrich Chemical Co., Milwaukee, WI). The reagent gases used were industrial-grade nitrogen and standard mixtures of nitric oxide (NO) in ultrapure nitrogen obtained from Airgas National Welders, Charlotte, NC. The water used to prepare the experimental solutions was purified using a Milli-Q Advantage A10 with Elix 5 system obtained from Millipore Corporation (Bedford, MA). The water had a resistivity of at least $18.2 \text{ M}\Omega \text{ cm}$ at 25°C , and TOC, silicates, and heavy metals contents were reduced to a very low parts-per-billion levels.

Experimental Procedure. The scrubbing system used for this work consisted of a jacketed bubble column reactor made of pyrex glass (5.1-cm i.d. \times 61-cm length; Ace Glass, Inc., Vineland, NJ), a flue gas blending system, and an analytical train as shown in Figure 1; it is similar to the one used in our previous studies.^{2,3} Flue gas blending was done using a Dynablender mass flow controller (Matheson Tri-Gas, Montgomeryville, PA) and two flow transducers calibrated to allow a maximum flow of 5 SLPM of gas. The simulated flue gas was introduced through a gas dispersion tube (Ace Glass, Inc.) fitted at the bottom of the scrubber and had a tube (8-mm o.d. \times 150-mm length) connected to a 25-mm-diameter disk at the discharge end. The disk had a porosity of grade C (25–50 μm). The reactor was designed to allow the gas to flow continuously in an upward direction, and the liquid phase could be operated either in batch or continuous mode. In these experiments, the scrubber was operated in semibatch mode; that is, the gas flowed upward continuously, and the liquid was stationary. The total

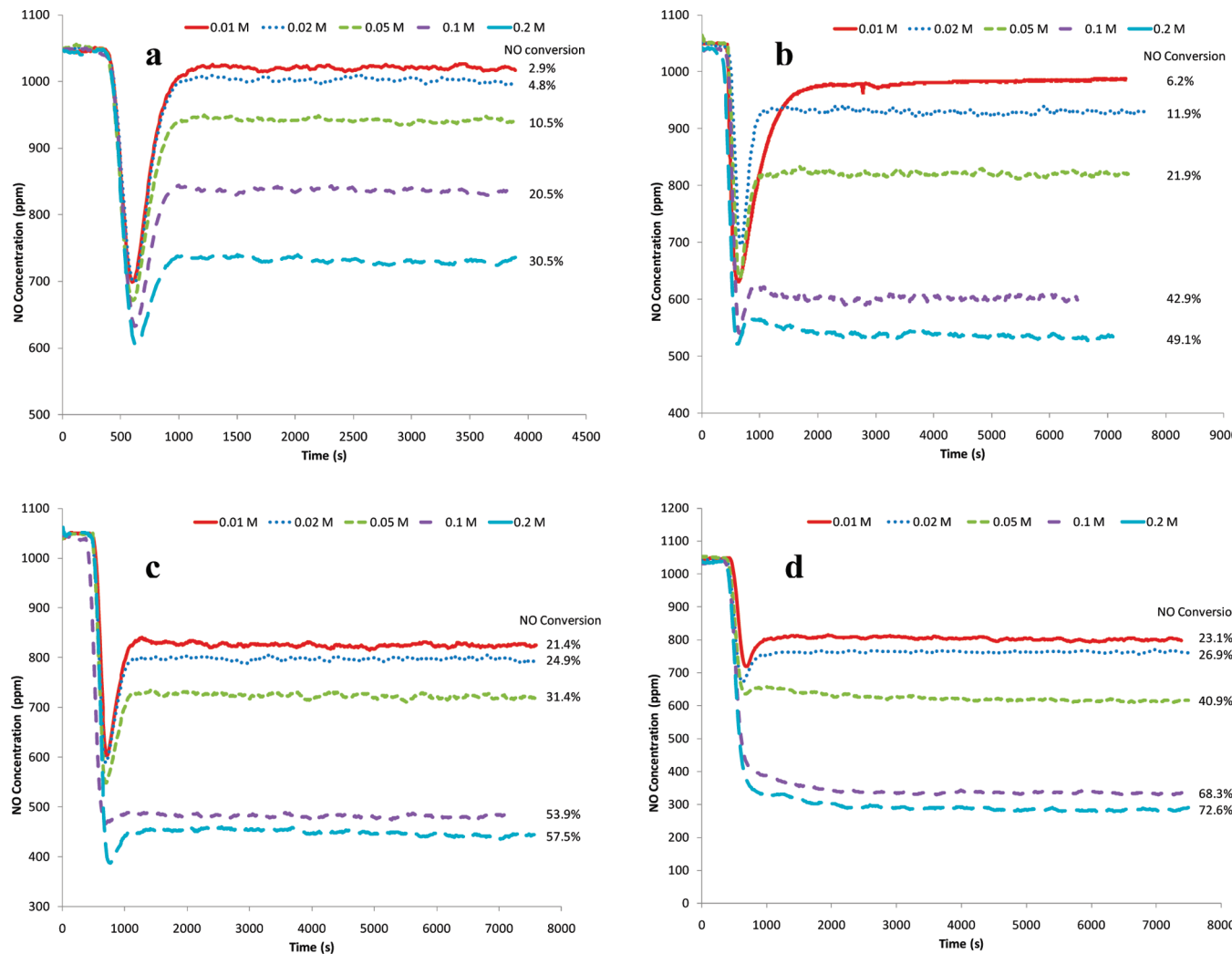


Figure 2. Nitric oxide concentration profile with time at different temperatures: (a) 30, (b) 40, (c) 50, and (d) 70 °C.

volume of scrubbing solution used was 1 L, corresponding to a liquid height of about 0.5 m.

The experiments were conducted at temperatures in the range of 23–90 °C, with each temperature maintained by means of cooling/heating water from a refrigerated cooler (Neslab RTE 7D1; Thermo Scientific, Waltham, MA). The column was filled initially with 750 mL of water, and the temperature was allowed to stabilize. Pure, dry nitrogen gas was then bubbled through the scrubber for at least 15 min to remove any dissolved oxygen; at the same time, the simulated flue gas was passed through the bypass line until a stabilized reading was obtained. Immediately before the start of the experiment, sodium persulfate, of the required quantity to make 1 L of the desired concentration of scrubbing solution, was added directly to the reactor, and water was then added to make the total volume 1 L. The dissolution of the persulfate was observed to be quick, aided by the warmth of the solution and the mixing action of the bubbling nitrogen. The appropriate quantity of buffer concentrate was also added to the solution to maintain the pH at the desired level. This was done to prevent the persulfate from being thermally activated long before the start of the experiment. Once the persulfate had fully dissolved and the solution became clear, the simulated flue gas was switched to the inlet of the reactor, and data acquisition was started.

The gas exiting from the reactor was passed through a condenser, cooled to 0.1 °C, to remove some of the moisture and then through a membrane dryer (MD-050-48P; Perma Pure

LLC, Toms River, NJ) to remove the remaining moisture so that it did not interfere with the analysis of the gas. Both the FTIR spectrometer and the membrane dryer were purged with dry, CO₂-free air from a laboratory gas generator (Parker Balston, Haverhill, MA) to continuously remove the moisture. The outlet concentration of NO_x from the bubble column was continuously monitored and recorded. The data were collected at 10-s intervals. The solution pH was measured before and after the experiment using an Accumet pH meter 50. The scrubbing solution was analyzed before and after each experiment using a Dionex ICS 3000 ion chromatographic system (Dionex Corporation, Sunnyvale, CA) for nitrates and nitrites. The gas phase was analyzed with an FTIR spectrometer (Tensor 27; Bruker Optics, Billerica, MA) equipped with a custom gas cell made by FTIR.com. The collection and analysis of the data were performed by the proprietary software, Enformatic FTIR Collection Manager (EFCM), from FTIR.com. Once the software had been calibrated with standards obtained from Airgas National Welders, it was able to perform online monitoring of the different species in the gas phase.

Results and Discussion

We conducted several sets of experiments at various temperatures [23, 30, 40, 50, 60, 70, and 90 °C (± 1 °C)] and persulfate concentrations [0.01, 0.02, 0.05, 0.1, and 0.2 M ($\pm 0.5\%$)] to investigate the effect of persulfate concentration

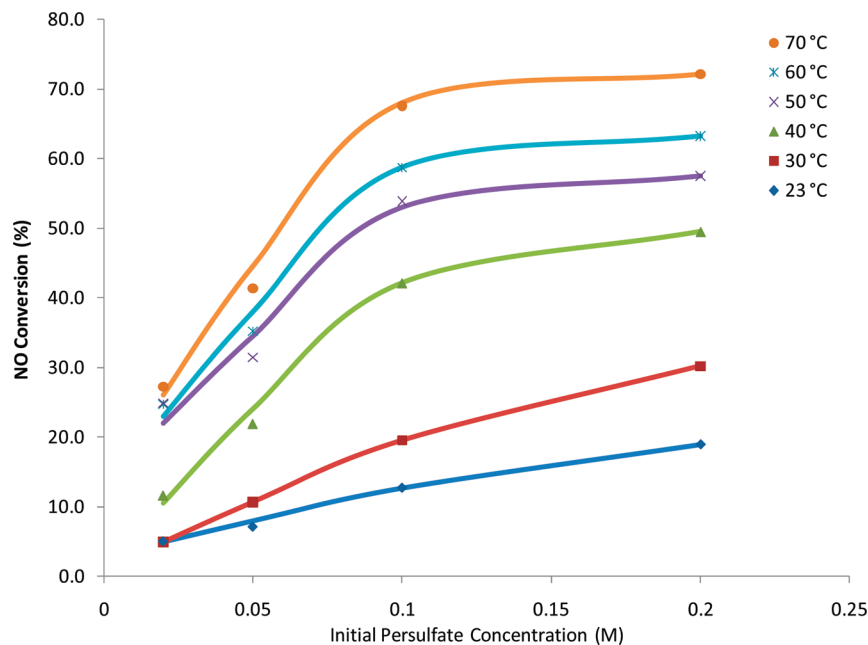


Figure 3. Dependence of NO conversion on persulfate concentration at different temperatures.

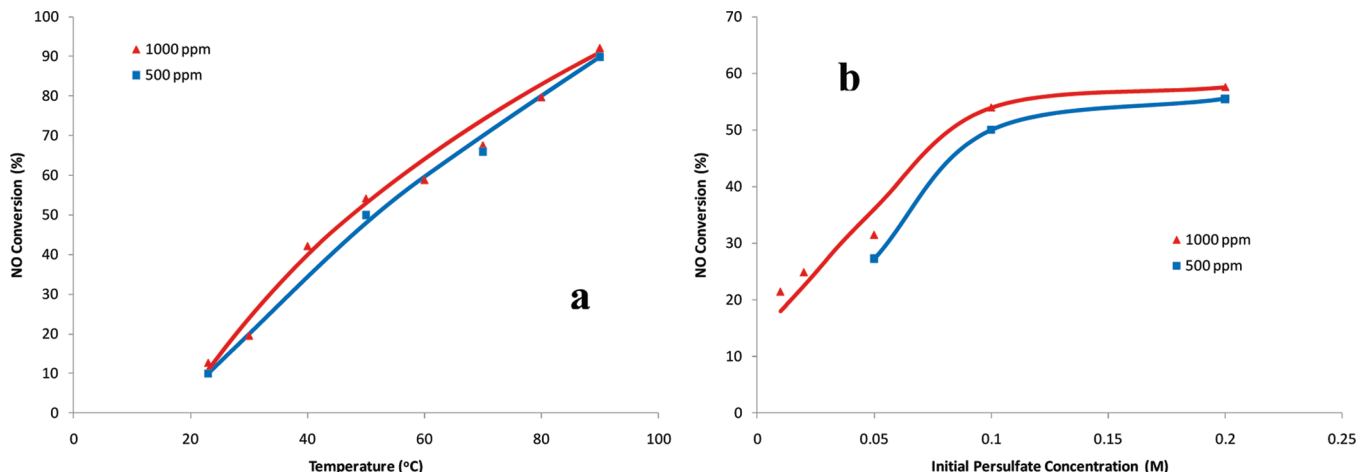


Figure 4. Effect of inlet NO concentration on (a) NO conversion at 0.1 M persulfate and (b) NO conversion at 50 °C.

on NO removal at different temperatures. Figure 2 illustrates the NO concentration as a function of time at some of the temperatures and persulfate concentrations studied. The curves show a dip in the beginning, corresponding to absorption in an unsaturated solution and mixing with nitrogen in the column headspace. For lower concentration and temperature levels, the initial drop in NO concentration (i.e., high absorption rate) could not be maintained, and the concentration returned to a higher value and remained steady for the rest of the experimental duration. On the other hand, NO concentration profiles at relatively higher temperatures and concentrations of persulfate showed no such decrease in absorption rate after the initial drop in NO concentration. In fact, the absorption rate continued to increase, and the NO concentration leveled off at much lower values for these conditions. A steady-state outlet concentration for the entire duration of the experiment indicates that, for all persulfate concentrations, the absorption capacity of the scrubbing solution was sufficient to maintain a constant absorption rate throughout the experiment without depleting significantly.

The fractional conversion of NO was calculated using the final steady-state value according to the expression

$$X_{\text{NO}} = \frac{[\text{NO}]_{\text{in}} - [\text{NO}]_{\text{out}}}{[\text{NO}]_{\text{in}}} \times 100 \quad (4)$$

where NO_{in} and NO_{out} are the steady-state concentrations [in parts per million (ppm)] of NO at the inlet and outlet of the bubble column, respectively. The effects of temperature and persulfate concentration on the fractional conversion of NO are illustrated in Figures 3 and 4, respectively. For example, the fractional conversions of NO were found to be 69% and 92% at 70 and 90 °C, respectively. Figure 3 shows the fractional conversion as a function of persulfate concentration for all temperatures up to 70 °C. At the lower temperatures of 23 and 30 °C, the fractional conversion is seen to increase almost linearly for the whole range of persulfate concentration. However, at higher temperatures, the proportional increase of fractional conversion with persulfate is observed only up to the persulfate concentration of 0.1 M. Beyond this level, a change in the concentration of persulfate did not induce a proportional change in fractional conversion. To be certain about this dependence, experiments were conducted at 60 °C for persulfate concentrations up to 1.0 M. The data are shown in Figure 5.

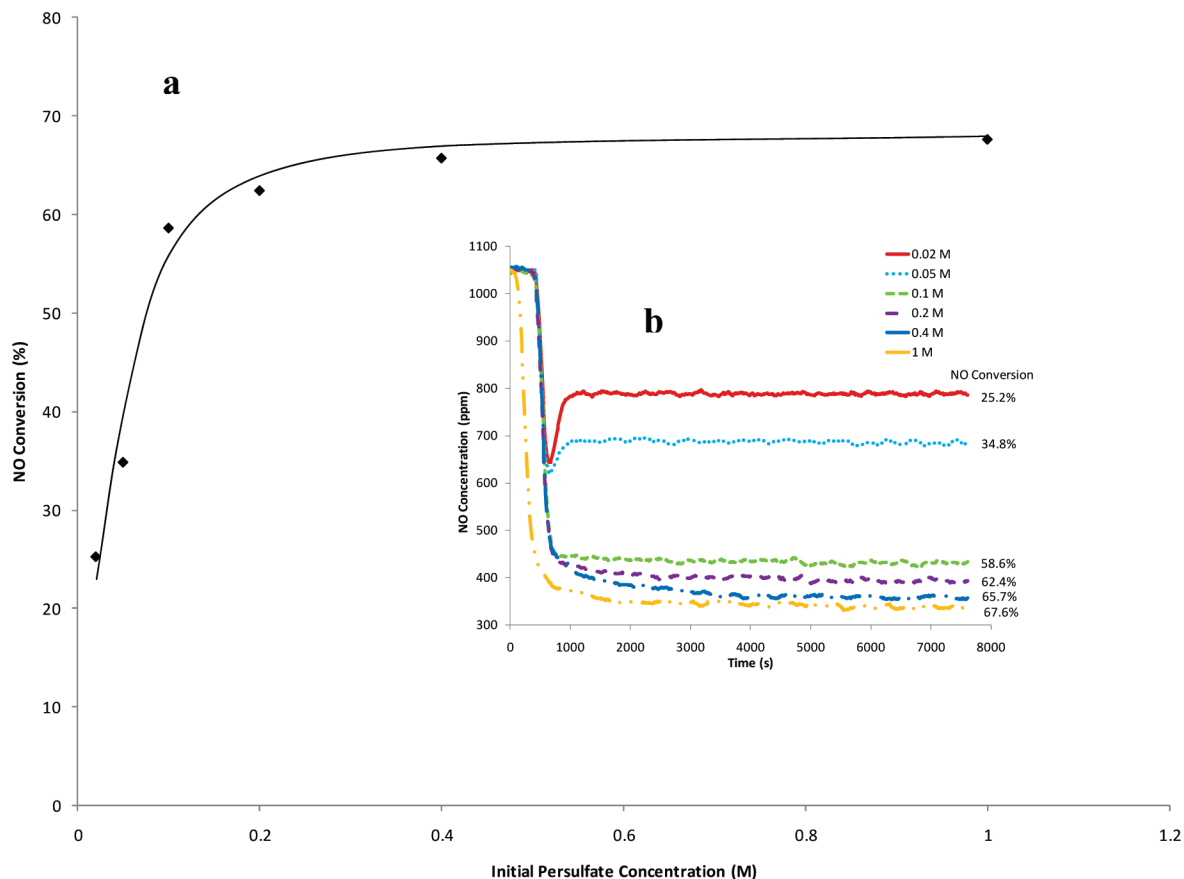
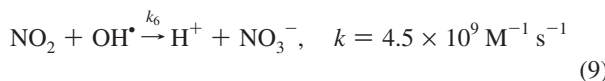
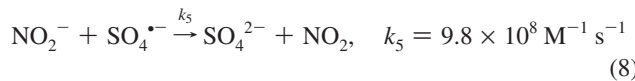
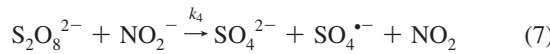
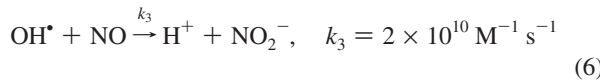
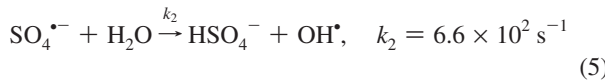


Figure 5. Dependence of NO conversion on persulfate concentration at 50 °C: (a) NO conversion vs persulfate concentration, (b) NO concentration profiles at different persulfate concentrations.

House¹¹ presented an exhaustive review on the mechanisms of persulfate decomposition under different conditions. Through convincing arguments, it was demonstrated that the chain-reaction mechanism presented by Bartlett and Cotman¹⁷ for uncatalyzed decomposition of persulfate is the most probable one. This mechanism is readily extendable to the case in which an oxidizable substance is present in the aqueous phase (in which case the decomposition rates have been found to be higher).¹¹ Based on this mechanism, we can assume that the following set of reactions (with their corresponding rate constants¹⁸) coupled with eq 2 are responsible for consumption of NO:

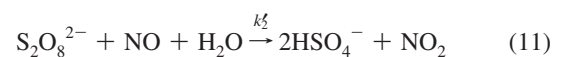


Using the pseudo-steady-state approximation (PSSA) and considering $\text{SO}_4^{\bullet-}$ and NO_2^- as intermediates, this mechanism results in a first-order rate expression in persulfate concentration for the consumption of NO in the liquid phase (derivation of

eq 10 shown in the Supporting Information).

$$\left(\frac{dC_{\text{NO}}}{dt} \right)_{\text{reaction}} = -(k_1 + k_4 C_{\text{NO}_2^-}) C_{\text{S}_2\text{O}_8^{2-}} = -k'_1 C_{\text{S}_2\text{O}_8^{2-}} \quad (10)$$

Thus, the degradation of NO is first-order with respect to persulfate concentration, and the linearity of the NO fractional conversion with respect to the persulfate concentration (at least up to 0.1 M) at all temperatures (Figure 3) becomes apparent. We can also conclude that the absorption of NO is kinetically controlled up to a persulfate concentration of 0.1 M and, above this concentration, reaction kinetics has little effect on NO absorption. Equation 10 can also be modified to include the direct oxidation of NO by persulfate, which might not be as significant as the radical reactions. At neutral pH (3–7), the reduction of persulfate leads to the generation of two bisulfite ions and oxygen,¹⁹ and therefore, reaction 11 is also possible



The overall oxidation of NO by persulfate is then given by the equation

$$\begin{aligned} \left(\frac{dC_{\text{NO}}}{dt} \right)_{\text{reaction}} &= -(k_1 + k_4 C_{\text{NO}_2^-}) C_{\text{S}_2\text{O}_8^{2-}} - k'_2 C_{\text{NO}} C_{\text{S}_2\text{O}_8^{2-}} = \\ &- k'_1 C_{\text{S}_2\text{O}_8^{2-}} - k'_2 C_{\text{NO}} C_{\text{S}_2\text{O}_8^{2-}} \end{aligned} \quad (12)$$

and the rate of persulfate consumption is given by

$$\frac{dC_{\text{S}_2\text{O}_8^{2-}}}{dt} = -k'_1 C_{\text{S}_2\text{O}_8^{2-}} - k'_2 C_{\text{NO}} C_{\text{S}_2\text{O}_8^{2-}} \quad (13)$$

It is important to offer plausible explanation for the coupled effects of persulfate concentration and temperature on the fractional conversion of NO. At lower temperatures, the fractional conversion of NO appears to be linearly proportional to persulfate at lower persulfate concentrations. From the evidence in the literature, oxidation in persulfate solution occurs through reaction with the free radicals generated by the decomposition of persulfate.²⁰ It is fairly obvious that, at higher temperatures, the decomposition of persulfate is faster, and so is the rate of generation of oxidative species. However, higher temperatures combined with higher persulfate concentrations, for which higher production of sulfate radicals is expected, result in a lower rate of change in the fractional conversion, and the almost-linear increase in NO fractional conversion with persulfate concentration is no longer observed. This is possibly due to self-recombination and intercombination of oxidative sulfate and hydroxyl ($\text{SO}_4^{\cdot-}$ and OH^{\cdot}) free radicals with the net effect of decreasing the conversion reaction rates.^{6,11}

In general, there are two ways in which NO can be removed by wet processes. One is the oxidation of NO to NO_2 in the gas phase prior to absorption into the liquid phase. The other is the absorption of NO in the liquid phase and subsequent consumption by a chemical oxidant. The presence of oxygen and water in the gas phase establishes a rapid equilibrium among NO, NO_2 , and other NO_x species. The gas-phase processes can be represented by the following reactions²¹

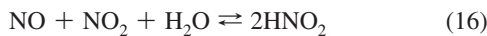


Figure 6 shows the gas-phase FTIR analysis for representative inlet and outlet spectra and for the standard spectra used for calibration. As indicated in this figure, the NO bands appear in the region between 1825 and 1949 cm^{-1} , and the water bands appear in the two regions between 1446 and 1754 cm^{-1} and between 3617 and 3878 cm^{-1} . These regions were specified in EFCM along with the corresponding concentrations for online monitoring of NO concentration. NO_2 absorbs at about 1600 cm^{-1} , N_2O_5 at 1246 and 1720 cm^{-1} , and HNO_3 at 1326 cm^{-1} . Our FTIR data showed no peaks in these regions except those of water vapor, indicating that probably no other NO_x species formed in significant amounts in the gas phase, excluding the possibility of any gas-phase reactions.

The analysis of liquid samples taken every 10 min during an experimental run revealed the presence of nitrate, nitrite, and sulfate, along with phosphate (retention time = 7.977 min) and a small amount of chloride (retention time = 3.057 min) (Figure 7). Phosphate ions came from the buffer used, and chloride probably came from the pH probe, which contained KCl solution. The quantity of chloride ion was too small to have any effect on the system. The nitrite, nitrate, and sulfate ions eluted within close proximity of each other. The quantity of sulfate ions, being very high compared to the amounts of other ions, presented a difficulty in the measurement of nitrates, which eluted at the tail of the sulfate peak. The samples had to be diluted to keep the sulfate peak low, but this might have introduced some error in the amounts of nitrate and nitrite. The high conductivity of the phosphate ions also interfered with the measurements, increasing the baseline between injections and possibly acting as a secondary eluent ion. The material balance for N at 40 and 60 °C, carried out using analysis

of the scrubbing solution at the beginning and end of each run of 2 h, is presented in Table 1 (sample calculation in Supporting Information). The total amount of N measured in solution (in the form of nitrate and nitrite) was found to be relatively higher than the amount of NO available from the gas phase (calculated using the ideal gas law). This is probably due to the errors introduced in the measurement of nitrates and nitrites for the reasons already discussed. These factors are supposed to cause the NO_2^- and NO_3^- concentration to be higher, which is consistent with our observation. However, it is interesting to note that the ratio of number of the moles of N in the liquid phase to the number of moles of NO coming from the gas is constant for a specific temperature. This indicates that the observed differences are dependent on the temperature and are not just random errors. This makes sense because the amount of sulfate is higher at higher temperature (because of increased decomposition of persulfate), which causes the amount of NO_3^- to be higher overall. Once these difficulties associated with the analysis of the liquid phase are overcome, the material balance will be expected to agree within reasonable accuracy. However, examination of the relative values of nitrite and nitrate in Table 1 reveals some interesting results. At low temperature (40 °C) and low concentrations of persulfate, the amount of nitrite formed was much larger (about 10 times) than the amount of nitrate formed, whereas at higher concentration (0.2 M), the formation of nitrate was about twice that of nitrite. At the higher temperature of 60 °C, barely any nitrite formed; in fact, whatever nitrite had been in the system at the beginning was converted to nitrate. It is evident that, at lower temperatures, the oxidation of dissolved NO was not complete, even at high persulfate concentrations, where significant amounts of nitrite remained. At higher temperatures, however, the oxidation was complete, and no trace of NO_2^- was found.

Effect of NO Concentration. The results in Figure 4a also illustrate the effects of temperature on fractional NO conversion for two initial NO gas-phase concentrations (500 and 1000 ppm) at a constant persulfate concentration of 0.1 M, and Figure 4b shows the effects of different initial persulfate concentrations at 50 °C for the same initial concentration of NO. It is expected that some concentration dependency should be observed, as a higher gas-phase NO concentration should result in higher NO liquid-phase concentrations and, hence, a higher liquid-phase reaction rate. As expected, fractional conversions at 1000 ppm NO were slightly more than those at 500 ppm NO at all initial concentrations of persulfate studied. However, when the persulfate concentration was constant and only temperature was varied, the difference in NO fractional conversion was marginal. On the other hand, the NO concentration had more of an effect on the fractional conversion when the persulfate concentrations were varied and the temperature was kept constant. This is to be expected, given that the absorption of NO is mostly controlled by the reactions in the liquid phase. However, the results also appear to indicate that, when the NO concentration was too much higher than nominal, too many solute (i.e., NO) molecules were competing for the persulfate-generated hydroxyl radicals to produce NO_2^- . However, in the presence of a lean concentration of NO, it appears that the tendency for the hydroxyl and sulfate radicals to recombine and intercombine predominated over interaction with the fewer solute species. We noticed similar trends in our previous study on the sonochemical oxidation of NO, which is also initiated by OH^{\cdot} , where these effects were explained in more detail.²²

Model. A simple model has been developed based on the aforementioned results to correlate with experimental data. The main

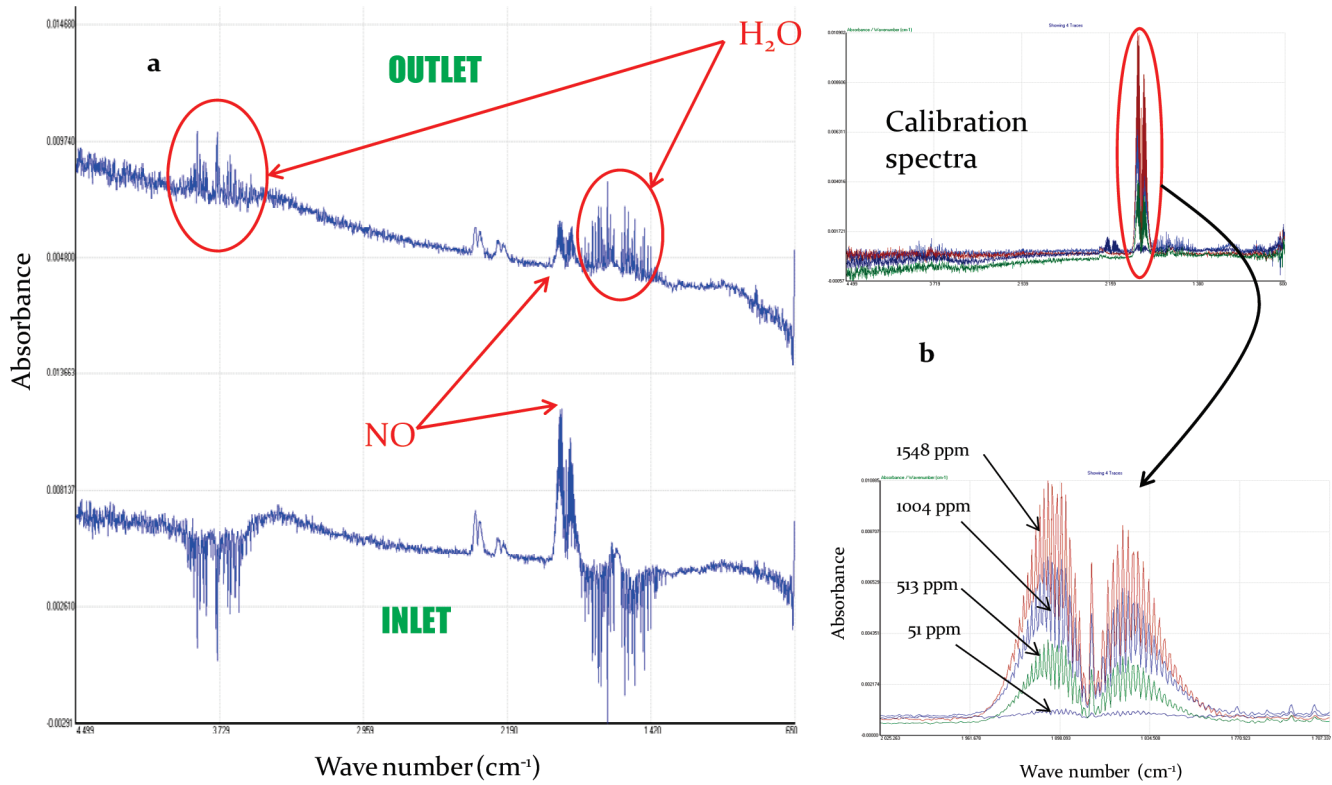


Figure 6. (a) Representative FTIR spectra at the inlet and outlet of the reactor at the end of an experimental run. (b) Standard spectra used for the calibration of the FTIR data collection software.

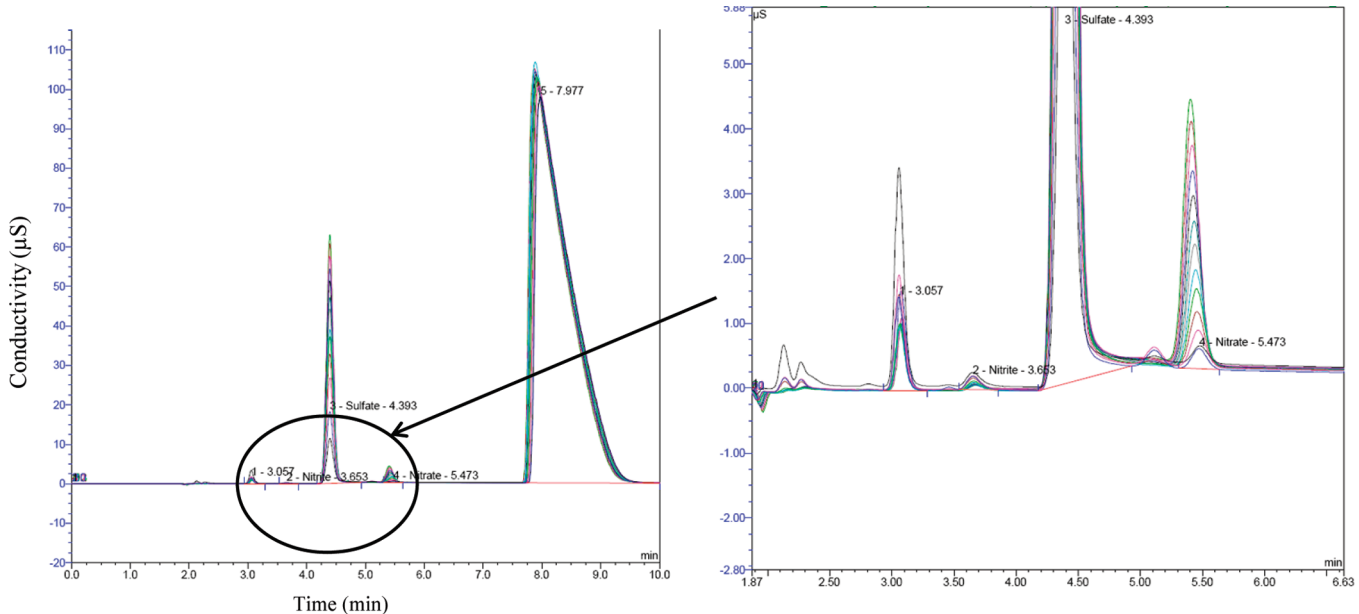


Figure 7. Ion chromatograph peaks for samples taken at 10-min interval (temperature = 60 °C, persulfate concentration = 0.02 M, NO concentration = 1040 ppm, gas flow rate = 0.1 SLPM).

assumptions of the model are that the gas and liquid are completely back-mixed and the transfer of NO from gas to liquid is liquid-phase-controlled.

The rate of transfer of NO from gas to liquid, using film theory, is given by

$$R_A = K_L a \left(\frac{P_{\text{NO}}}{H} - C_{\text{NO}} \right) \quad (18)$$

where $K_L a$ is the mass-transfer coefficient, H is the Henry's law coefficient, P_{NO} is the partial pressure of NO at the outlet,

and C_{NO} is the aqueous concentration of NO. P_{NO} is calculated as $P_{\text{NO}} = \text{ppm}_{\text{NO}} \times 10^{-6} \times P_{\text{total}}$, where P_{total} is 1 atm and ppm_{NO} is the NO concentration in molar parts per million. The material balance of NO in the gas phase yields

$$\frac{V_G}{RT} \frac{dP_{\text{NO}}}{dt} = \frac{Q}{RT} (P_{\text{NO}}^{\text{in}} - P_{\text{NO}}) - R_A V_L \quad (19)$$

where V_G is the gas holdup volume, R is the gas constant, T is the temperature, Q is the gas flow rate, $P_{\text{NO}}^{\text{in}}$ is the partial

Table 1. Nitrogen Balance Showing the Amount Available from the Gas Phase and That Found in the Liquid Phase

temperature (°C)	persulfate concentration (M)	inlet NO (ppm)	outlet NO (ppm)	time (min)	total N from gas phase (mmol)	change in nitrate, ΔNO_3^- (mmol)	change in nitrite, ΔNO_2^- (mmol)	ΔN in solution (mmol)	$(\Delta\text{N in solution})/(N \text{ from gas phase})$
40	0.02	1004	866	120	0.0737	0.00929	0.1034	0.1127	1.53
40	0.05	1004	707	120	0.1592	0.02086	0.2166	0.2375	1.49
40	0.2	1004	515	120	0.2619	0.2709	0.1351	0.4060	1.55
60	0.0217	1004	756	120	0.1328	0.2273	0.00	0.2273	1.71
60	0.05	1004	426	120	0.3098	0.5812	-0.01821	0.5629	1.82
60	0.2	1004	345	120	0.3528	0.6748	-0.07162	0.6032	1.71

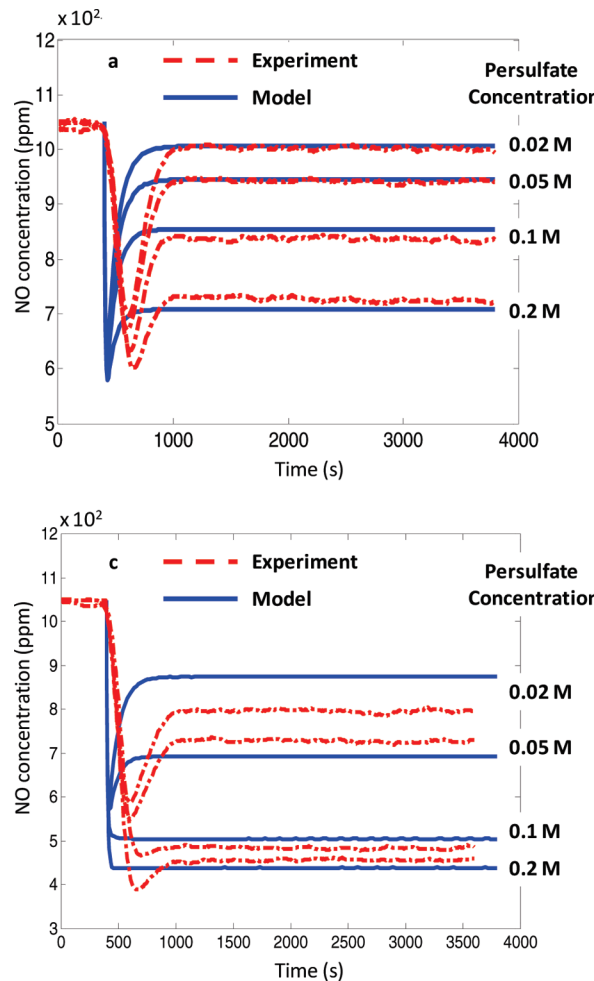
pressure of NO at the inlet, and V_L is the liquid volume. Substituting eq 18 into eq 19 gives

$$\frac{dP_{\text{NO}}}{dt} = \frac{Q}{V_G}(P_{\text{NO}}^{\text{in}} - P_{\text{NO}}) - \frac{V_L RT}{V_G} K_{\text{La}} \left(\frac{P_{\text{NO}}}{H} - C_{\text{NO}} \right) \quad (20)$$

From eqs 12 and 18, the material balance for aqueous NO yields the equation

$$\frac{dC_{\text{NO}}}{dt} = K_{\text{La}} \left(\frac{P_{\text{NO}}}{H} - C_{\text{NO}} \right) - k'_1 C_{\text{S}_2\text{O}_8^{2-}} - k'_2 C_{\text{NO}} C_{\text{S}_2\text{O}_8^{2-}} \quad (21)$$

Equations 20 and 21 were solved simultaneously with eq 13 using Matlab with varying values of the parameters K_{La} , k'_1 , and k'_2 until a good fit for the data was obtained. Figure 8 shows the experimental and model plots at different temperatures. It is obvious that this simple model adequately fits our experimental data. The final value of K_{La} is $2.83 \times$



10^{-2} s^{-1} , and the values of k'_1 and k'_2 at various temperatures are reported in Table 2, along with their respective activation energies. To calculate the activation energies for the rate constants k'_1 and k'_2 , the values obtained at different temperatures were used to generate an Arrhenius plot based on the equation

$$\ln\left(\frac{k}{k_{30^\circ\text{C}}}\right) = -\frac{E}{RT} + \frac{E}{RT_{30^\circ\text{C}}} \quad (22)$$

with the y axis being $(\ln k)/k_{30^\circ\text{C}}$ and the x axis being $1/T$. The plots are shown in Figure 9.

Effect of pH. The effect of pH was studied at a persulfate concentration of 0.1 M and at the three temperatures 23, 50, and 70 °C (Figure 10). For these experiments, the solutions were initially buffered, and NaOH was continually added to the reactor during each experiment as needed to maintain the pH at a constant level. No significant effect was noticed at the lower temperatures of 23 and 50 °C. However, at 70 °C, a considerable

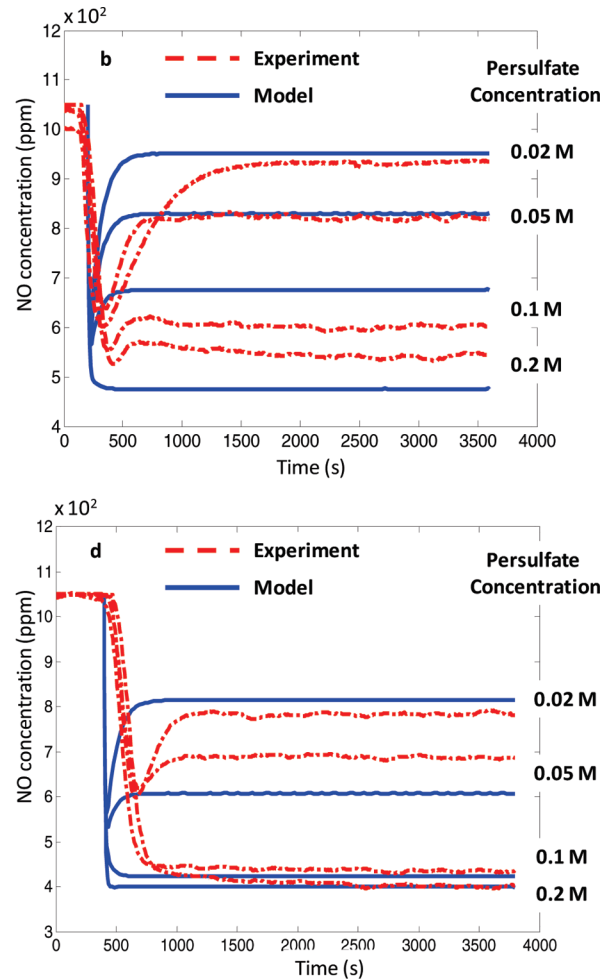


Figure 8. Experimental data and model predictions for different persulfate concentrations at different temperatures: (a) 30, (b) 40, (c) 50, and (d) 60 °C.

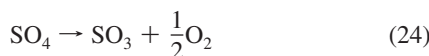
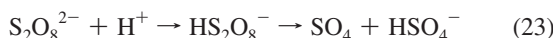
Table 2. Rate Constants at Different Temperatures Obtained from Model Fit of the Experimental Data

temperature (°C)	k'_1 (s ⁻¹)	k'_2 (M ⁻¹ s ⁻¹)
30	2.50×10^{-8}	2.00×10^{-2}
40	5.00×10^{-8}	5.00×10^{-2}
50	9.00×10^{-8}	1.00×10^{-1}
60	1.00×10^{-7}	1.50×10^{-1}

^a Activation energy = 40238.9 J/mol. ^b Activation energy = 56883.1 J/mol.

improvement in conversion was observed at pH 9: the steady-state concentration of NO dropped from 330 ppm at pH 7 to about 260 ppm at pH 9, although we saw no change going from pH 9 to pH 12.

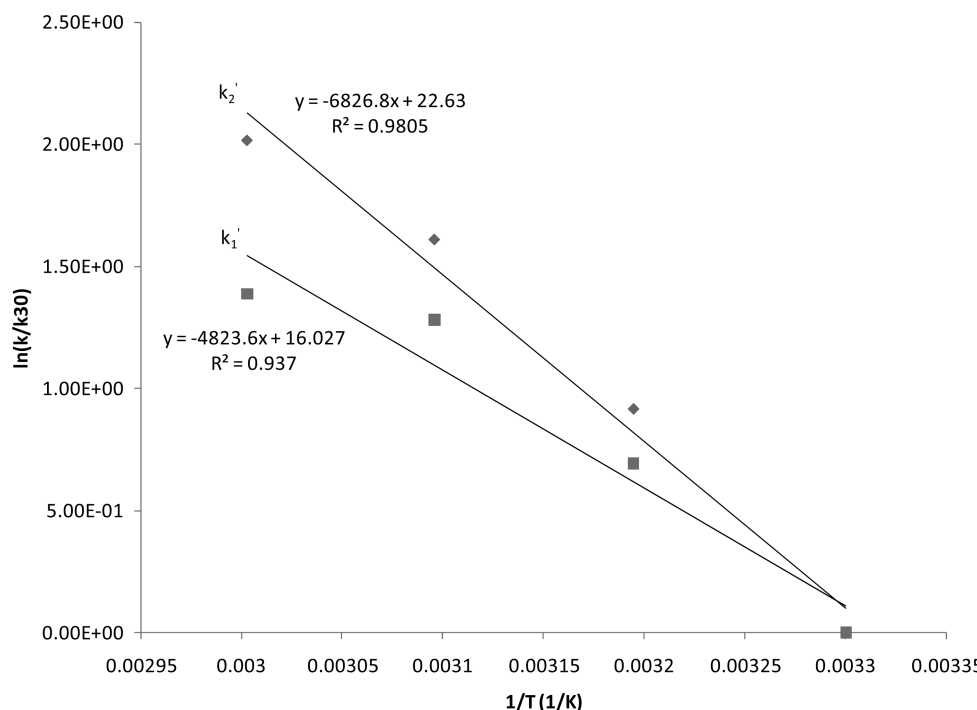
It is generally believed^{11,23,24} that the acid-catalyzed decomposition of persulfate follows the mechanism proposed by Kolthoff and Miller²⁵



In strong acid

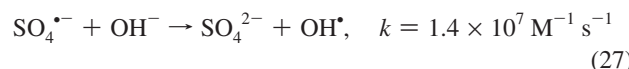


The difference between the acid-catalyzed decomposition mechanism and the uncatalyzed decomposition mechanism given before is quite obvious. The uncatalyzed decomposition occurs via the symmetrical breakup of persulfate ion into two SO_4^{2-} radicals, which, upon reacting with water, produce OH^\bullet radical and liberate oxygen. On the other hand, the acid-catalyzed decomposition does not produce any reactive radical species. It is assumed that, in aqueous solutions of persulfate, both uncatalyzed and acid-catalyzed reactions occur simultaneously, also yielding a first-order rate expression²⁵

**Figure 9.** Arrhenius plot of rate constants.

Thus, a decrease in solution pH will accelerate the persulfate decomposition but will not produce an increase in the amount of reactive radicals generated. We should not, therefore, see a change in NO absorption rate at low pH.

Alkaline pH has been found to be very effective in the persulfate-induced degradation of groundwater contamination.²⁶ Liang and co-workers investigated the effect of pH on trichloroethylene (TCE) degradation by persulfate.²⁷ They found that neutral to alkaline conditions are much more effective in TCE degradation than acidic conditions. They also investigated the effect of pH on the relative production of SO_4^{2-} and OH^\bullet radicals upon persulfate degradation by a chemical probe method.²⁸ The rate of persulfate degradation was found to be much higher at high pH (~12), and the dominant radical species at this pH was found to be OH^\bullet radical. Electron spin resonance (ESR) spin trapping studies^{29–31} have shown that alkaline conditions can induce the mechanism of radical interconversion of SO_4^{2-} to OH^\bullet by the reaction²⁸



Although eq 5 produces OH^\bullet radicals at all pH values, its rate is quite low ($k[\text{H}_2\text{O}] < 2 \times 10^{-3} \text{ s}^{-1}$ ^{29,32}), whereas eq 27 is quite fast under alkaline conditions. From a comparison of the rate constants of SO_4^{2-} and OH^\bullet radicals with certain organic substances presented by Liang et al.,²⁸ it is apparent that OH^\bullet radical is the more reactive of the two species. Moreover, because OH^\bullet reacts with NO at an almost diffusion-controlled rate ($k = 2 \times 10^{10} \text{ M}^{-1} \text{ s}^{-1}$),³³ we could safely conclude that the consumption of NO in the liquid phase is much higher under alkaline than acidic conditions, which explains the results obtained in this study. However, at very high pH, the effectiveness might be reduced because of the rapid dissociation of OH^\bullet .

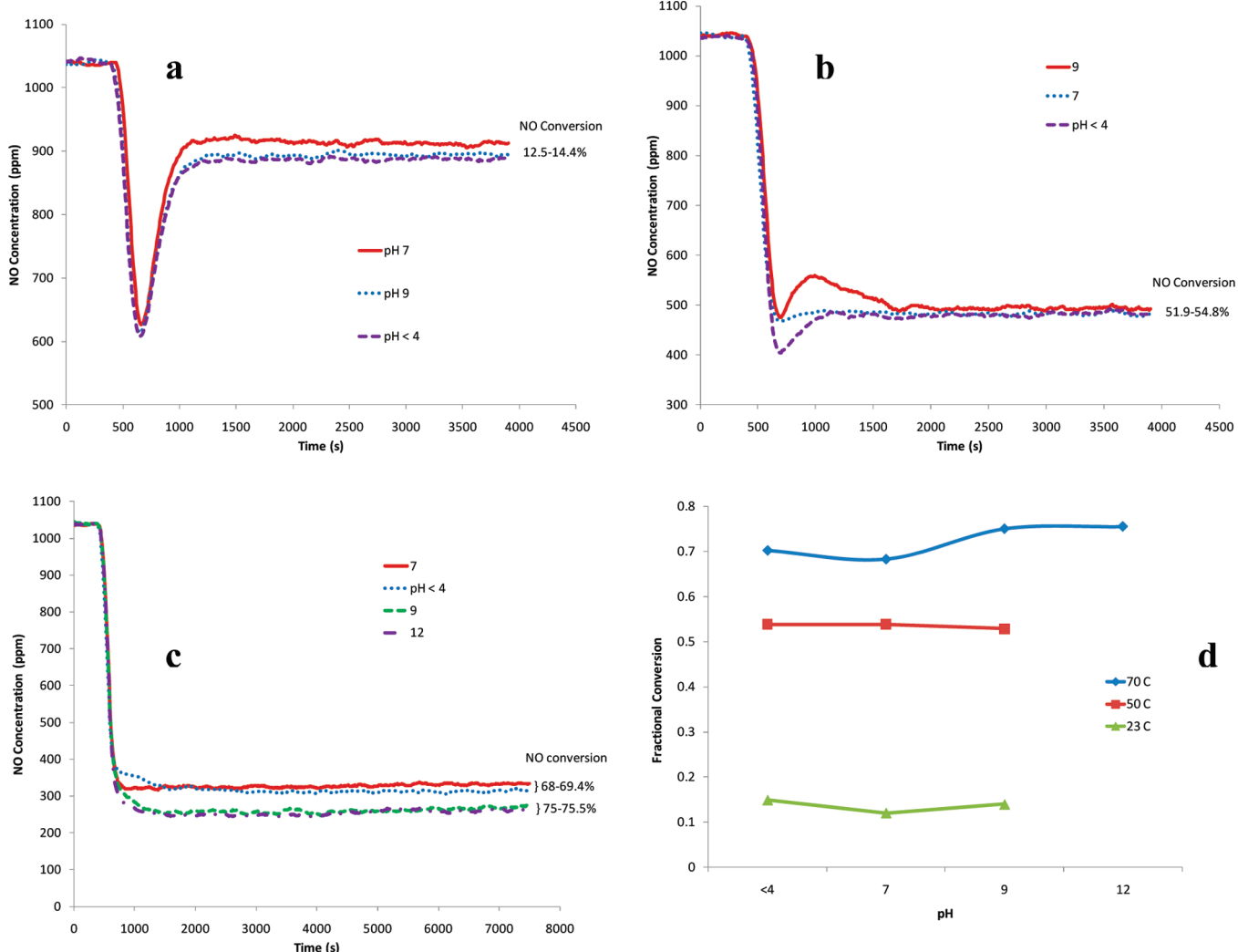
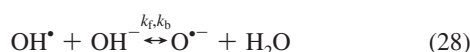


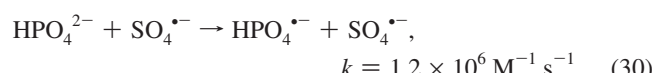
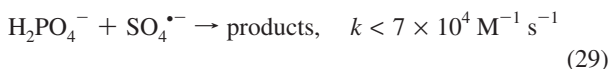
Figure 10. Effect of pH at a persulfate concentration of 0.1 M: NO concentration profiles at (a) 23, (b) 50, and (c) 70 °C and (d) NO fractional conversion at different pH values and temperatures.

in alkaline solutions, as illustrated by the equation



where $k_f = 1.2 \times 10^{10} \text{ M}^{-1} \text{ s}^{-1}$ for the forward reaction and $k_b = 9.3 \times 10^7 \text{ s}^{-1}$ for the backward reaction and the oxide radical ion ($\text{O}^{\bullet-}$) is known to react more slowly with the same substrate than OH^{\bullet} .³⁴

Finally, it is important to discuss the possible effects of the phosphate buffers used in the persulfate– NO_x system. In an earlier work, we discussed the role of phosphate in a sonochemical system containing OH^{\bullet} radicals and showed that the effect of phosphate should not be significant on the basis of the relative rates of the phosphate ions with the OH^{\bullet} radical compared with the rate of oxidation of NO_x species in solution by the OH^{\bullet} radicals.³⁵ Arguing along the same lines for persulfate, a similar conclusion would be obtained based on the following reaction rates¹⁸



These reactions are slower than those in eqs 6, 8, and 9, which have nearly diffusion-controlled rates. That is, the various phosphate species react with OH^{\bullet} and sulfate radicals at rates generally lower than the rates of reaction of OH^{\bullet} and $\text{SO}_4^{\bullet-}$ radicals with the NO_x species. Therefore, the competition for OH^{\bullet} and $\text{SO}_4^{\bullet-}$ could be expected to be least in the pH region of H_2PO_4^- and HPO_4^{2-} used in our buffer system; hence, the impact on our persulfate– NO_x system is expected to be minimal.³⁵ Liang and Bruell also showed that phosphate-buffered systems (e.g., phosphate anion species) do not have a significant effect on the persulfate oxidation of TCE.³⁶

Effect of Chloride. ClO_2 and NaClO_2 are two compounds of chlorine that have been studied quite extensively^{2,37–43} for the removal of NO_x and SO_2 and have been found to be quite effective.^{38–40} In our previous studies on the sonochemical oxidation of NO, positive effects of Cl^- ion were noticed.³⁵ In an advanced oxidation system such as thermally activated persulfate solution, the interaction between reactive free radicals such as $\text{SO}_4^{\bullet-}$ and OH^{\bullet} and Cl^- ion could generate interesting results. In view of this, we decided to perform a limited study of the effects of chloride ion on NO absorption using aqueous persulfate solutions. Figure 11 shows the results of adding NaCl

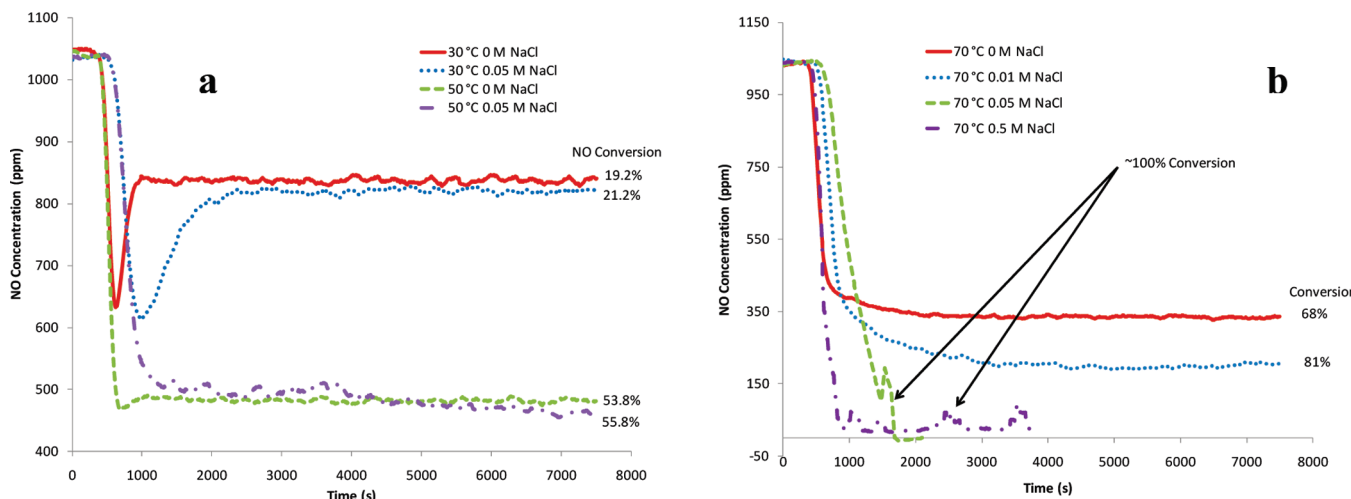
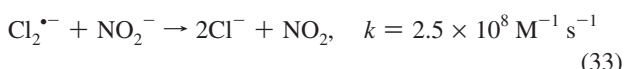
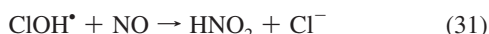


Figure 11. Effect of chloride at a persulfate concentration of 0.1 M: NO concentration profiles showing the effects of (a) the presence and absence of 0.05 M of NaCl at 30 and 50 °C and (b) different concentrations of NaCl at 70 °C.

to 0.1 M sodium persulfate solutions at three temperature levels (30, 50, and 70 °C). At the lower temperatures of 30 and 50 °C, introduction of 0.05 M of NaCl had little effect, similar to the observation made for the case of pH effect. However, at 70 °C, even a concentration of 0.01 M chloride had a very pronounced effect, where the conversion of NO went from 68% without any NaCl to 81% with NaCl. Upon addition of higher quantities of NaCl (0.05 and 0.5 M), quite dramatic effects were observed in that we could find no trace of NO in the FTIR spectrum and a variety of other peaks appeared. Introduction of Cl⁻ ion into the activated persulfate system can start a host of other reactions.^{35,44,45}

It is well-known that a large number of chlorinated reactive radicals (Cl[•], ClOH[•], Cl₂^{•-}) are formed through complex reactions involving chloride ion and OH radical.^{18,35} The chlorinated radicals formed from these reactions are capable of launching rapid attack on dissolved NO, forming nitrates and nitrites, as shown in the equations^{18,35}



Although their reactivities might be lower than those of sulfate and hydroxyl radicals, these species enhance the NO removal efficiency of the system by increasing the total number of reactive radical species available for reaction. These radicals are also capable of scavenging some of the sulfate and hydroxyl radicals, but it seems that the concentration of persulfate is sufficient to maintain a steady supply of these radicals. It can be seen from Figure 3 that increasing the temperature of the system at the same persulfate level results in an increased conversion of NO. This means that thermal activation simply enhances the rate of generation of reactive radicals at the same persulfate concentration. This is the same function as performed by chloride ion and the subsequent species in this case.

Conclusions

The absorption of NO by aqueous solutions of persulfate (0.01–0.2 M) has been studied for the first time in a bubble column reactor at various temperatures (23–90 °C). For 0.1 M

persulfate solution, the fractional conversions of NO using feed concentration of about 500 and 1000 ppm were found to be 69% and 92% at 70 and 90 °C, respectively. It was generally observed that NO conversion increased with increasing temperature and persulfate concentration. However, above about 0.1 M persulfate, there was little change in NO conversion with increasing persulfate concentration. The absorption of NO by persulfate solution is thought to be dependent on the reaction of dissolved NO with the reactive radicals generated by thermal activation of persulfate. The consumption of NO by reactions in the liquid phase maintains the driving force needed for absorption. Acidic pH does not influence the rate of absorption of NO, whereas at pH ≥ 9, an increase in NO conversion occurs at higher temperatures. Chloride ions have a dramatic effect on the system, again at higher temperatures. Even a small quantity of NaCl produces a significant increase in conversion, and at larger concentrations of chloride ions, NO appears to be completely removed. Chloride is assumed to start a chain of reactions producing other reactive radicals and species that enhance the efficiency of absorption by reacting with NO. Studies at different NO concentrations showed no significant change as the absorption is mainly liquid-phase-controlled. The findings of these preliminary studies suggest that the use of persulfate as a possible oxidant for the wet scrubbing of NO is very promising. Further work will be done on this persulfate–NO system to investigate the effects of other parameters (such as the presence of SO₂, CO₂, O₂, and other flue gas components; the gas and liquid flow rates; the use of different additives) in more detail and to find the mass-transfer and kinetic parameters related to this system. Because of the low cost and environmentally benign nature of persulfate compared to other chemical oxidants, it might be economical to use aqueous persulfate for the removal of NO_x in gas–liquid contactors.

Acknowledgment

The authors acknowledge the funding received from the National Science Foundation (NSF) for financial assistance via Grant CBET-0651811.

Supporting Information Available: Derivation of eq 10 and sample calculation for nitrogen balance. This material is available free of charge via the Internet at <http://pubs.acs.org>.

Literature Cited

- (1) Power Plants, Pollution and Soot - Air Quality. Environmental Defense Fund, New York. <http://www.edf.org/page.cfm?tagID=78> (accessed May 20, 2010).
- (2) Adewuyi, Y.; He, X.; Shaw, H.; Lolertpihop, W. Simultaneous Absorption and Oxidation of NO and SO₂ by Aqueous Solutions of Sodium Chlorite. *Chem. Eng. Commun.* **1999**, *174*, 21–51.
- (3) Adewuyi, Y.; Owusu, S. Aqueous Absorption and Oxidation of Nitric Oxide with Oxone for the Treatment of Tail Gases: Process Feasibility, Stoichiometry, Reaction Pathways, and Absorption Rate. *Ind. Eng. Chem. Res.* **2003**, *42*, 4084–4100.
- (4) Liang, C.; Huang, C.-F.; Chen, Y.-J. Potential for Activated Persulfate Degradation of BTEX Contamination. *Water Res.* **2008**, *42*, 4091–4100.
- (5) Liang, C.; Chen, Y.-J.; Chang, K.-J. Evaluation of Persulfate Oxidative Wet Scrubber for Removing BTEX Gases. *J. Hazard. Mater.* **2009**, *164*, 571–579.
- (6) Liang, C.; Wang, Z.-S.; Mohanty, N. Influences of Carbonate and Chloride Ions on Persulfate Oxidation of Trichloroethylene at 20°C. *Sci. Total Environ.* **2006**, *370*, 271–277.
- (7) Bard, A.; Parsons, R.; Jordan, J. *Standard Potentials in Aqueous Solution*; Marcel Dekker, Inc.: New York, 1985.
- (8) Osgerby, I. T. ISCO Technology Overview: Do You Really Understand the Chemistry? In *Contaminated Soils, Sediments and Water*; Calabrese, E. J., Kostecki, P. T., Dragun, J., Eds.; Springer: New York, 2006.
- (9) Wardman, P. Reduction Potentials of One-Electron Couples Involving Free-Radicals in Aqueous Solution. *J. Phys. Chem. Ref. Data* **1989**, *18*, 1637–1755.
- (10) Bard, A.; Faulkner, L. *Electrochemical Methods: Fundamentals and Applications*; John Wiley & Sons: New York, 2001.
- (11) House, D. A. Kinetics and Mechanism of Oxidations by Peroxydisulfate. *Chem. Rev.* **1962**, *62*, 185–203.
- (12) Antoniou, M. G.; de la Cruz, A. A.; Dionysiou, D. D. Degradation of Microcystin-Lr Using Sulfate Radicals Generated through Photolysis, Thermolysis and E-Transfer Mechanisms. *Appl. Catal., B* **2010**, *96*, 290–298.
- (13) Steiner, N.; Eul, W. Peroxides, Inorganic. In *Kirk-Othmer Encyclopedia of Chemical Technology*; Wiley: New York, 2006.
- (14) Rastogi, A.; Al-Abed, S. R.; Dionysiou, D. D. Sulfate Radical-Based Ferrous-Peroxymonosulfate Oxidative System for PCBs Degradation in Aqueous and Sediment Systems. *Appl. Catal., B* **2009**, *85*, 171–179.
- (15) Eaton, A. D.; Clesceri, L. S.; Rice, E. W.; Greenberg, A. E. *Standard Methods for the Examination of Water & Wastewater*; APHA, AWWA, and WEF: Washington, DC, 2005.
- (16) Sra, K. S.; Thomson, N. R.; Barker, J. F. Persistence of Persulfate in Uncontaminated Aquifer Materials. *Environ. Sci. Technol.* **2010**, *44*, 3098–3104.
- (17) Bartlett, P. D.; Cotman, J. D. The Kinetics of the Decomposition of Potassium Persulfate in Aqueous Solutions of Methanol. *J. Am. Chem. Soc.* **1949**, *71*, 1419–1422.
- (18) *NDRL/NIST Solution Kinetics Database*; National Institute of Standards and Technology: Gaithersburg, MD. <http://kinetics.nist.gov/solution> (accessed May 20, 2010).
- (19) *Persulfates—Technical Information*; FMC Corporation: Philadelphia, PA, 2001.
- (20) Huang, K.-C.; Couttenye, R. A.; Hoag, G. E. Kinetics of Heat-Assisted Persulfate Oxidation of Methyl *tert*-Butyl Ether (MTBE). *Chemosphere* **2002**, *49*, 413–420.
- (21) *NIST Chemical Kinetics Database*. National Institute of Standards and Technology: Gaithersburg, MD. <http://kinetics.nist.gov/kinetics/index.jsp> (accessed May 20, 2010).
- (22) Owusu, S.; Adewuyi, Y. Sonochemical Removal of Nitric Oxide from Flue Gases. *Ind. Eng. Chem. Res.* **2006**, *45*, 4475–4485.
- (23) Chandra Singh, U.; Venkataraao, K. Kinetics of Acid-Catalyzed and Ag(I) Catalyzed Decomposition of Peroxodisulfate in Aqueous Medium. *Int. J. Chem. Kin.* **1981**, *13*, 555–564.
- (24) Johnson, R. L.; Tratnyek, P. G.; Johnson, R. O. Persulfate Persistence under Thermal Activation Conditions. *Environ. Sci. Technol.* **2008**, *42*, 9350–9356.
- (25) Kolthoff, I.; Miller, I. The Chemistry of Persulfate. I. The Kinetics and Mechanism of the Decomposition of the Persulfate Ion in Aqueous Medium. *J. Am. Chem. Soc.* **1951**, *73*, 3055–3059.
- (26) Block, P.; Brown, R.; Robinson, D. Novel Activation Technologies for Sodium Persulfate *In Situ* Chemical Oxidation. Presented at the Fourth International Conference on the Remediation of Chlorinated and Recalcitrant Compounds, Monterey, CA, May 24–27, 2004.
- (27) Liang, C.; Wang, Z.-S.; Bruell, C. J. Influence of pH on Persulfate Oxidation of TCE at Ambient Temperatures. *Chemosphere* **2007**, *66*, 106–113.
- (28) Liang, C.; Su, H.-W. Identification of Sulfate and Hydroxyl Radicals in Thermally Activated Persulfate. *Ind. Eng. Chem. Res.* **2009**, *48*, 5558–5562.
- (29) Pennington, D. E.; Haim, A. Stoichiometry and Mechanism of Chromium(II)-Peroxydisulfate Reaction. *J. Am. Chem. Soc.* **1968**, *90*, 3700.
- (30) Hayon, E.; Treinin, A.; Wilf, J. Electronic Spectra, Photochemistry, and Autoxidation Mechanism of Sulfite–Bisulfite–Pyrosulfite Systems. The SO₂[−], SO₃[−], SO₄^{2−}, and SO₅^{2−} Radicals. *J. Am. Chem. Soc.* **1972**, *94*, 47.
- (31) Peyton, G. The Free-Radical Chemistry of Persulfate-Based Total Organic Carbon Analyzers. *Marine Chem.* **1993**, *41*, 91–103.
- (32) Norman, R.; Storey, P.; West, P. Electron Spin Resonance Studies. Part XXV. Reactions of Sulfate Radical Anion with Organic Compounds. *J. Am. Chem. Soc.* **1970**, *1087*–95.
- (33) Buxton, G.; Greenstock, C.; Helman, W.; Ross, A. Critical Review of Rate Constants for Reactions of Hydrated Electrons, Hydrogen Atoms and Hydroxyl Radicals (•OH/•O[−]) in Aqueous Solution. *J. Phys. Chem. Ref. Data* **1988**, *17*, 513–886.
- (34) Adewuyi, Y. G.; Appaw, C. Sonochemical Oxidation of Carbon Disulfide in Aqueous Solutions: Reaction Kinetics and Pathways. *Ind. Eng. Chem. Res.* **2002**, *41*, 4957–4964.
- (35) Adewuyi, Y.; Owusu, S. Ultrasound-Induced Aqueous Removal of Nitric Oxide from Flue Gases: Effects of Sulfur Dioxide, Chloride, and Chemical Oxidant. *J. Phys. Chem. A* **2006**, *110*, 11098–11107.
- (36) Liang, C.; Bruell, C. J. Thermally Activated Persulfate Oxidation of Trichloroethylene: Experimental Investigation of Reaction Orders. *Ind. Eng. Chem. Res.* **2008**, *47*, 2912–2918.
- (37) Brogren, C.; Karlsson, H. T.; Bjerle, I. Absorption of NO in an Aqueous Solution of NaClO₂. *Chem. Eng. Technol.* **1998**, *21*, 61–70.
- (38) Jin, D.-S.; Deshwal, B.-R.; Park, Y.-S.; Lee, H.-K. Simultaneous Removal of SO₂ and NO by Wet Scrubbing Using Aqueous Chlorine Dioxide Solution. *J. Hazard. Mater.* **2006**, *135*, 412–417.
- (39) Wei, J.-C.; Yu, P.; Cai, B.; Luo, Y.-B.; Tan, H.-Z. Absorption of NO in Aqueous NaClO₂/Na₂CO₃ Solutions. *Chem. Eng. Technol.* **2009**, *32*, 114–119.
- (40) Chien, T.-W.; Chu, H. Removal of SO₂ and NO from Flue Gas by Wet Scrubbing Using an Aqueous NaClO₂ Solution. *J. Hazard. Mater.* **2000**, *80*, 43–57.
- (41) Chu, H.; Chien, T.-W.; Twu, B.-W. The Absorption Kinetics of NO in NaClO₂/NaOH Solutions. *J. Hazard. Mater.* **2001**, *84*, 241–252.
- (42) Sada, E.; Kumazawa, H.; Kudo, I.; Kondo, T. Absorption of NO in Aqueous Mixed Solutions of NaClO₂ and NaOH. *Chem. Eng. Sci.* **1978**, *33*, 315–318.
- (43) Sada, E.; Kumazawa, H.; Kudo, I.; Kondo, T. Absorption of Lean NO_x in Aqueous Solutions of NaClO₂ and NaOH. *Ind. Eng. Chem. Process Des. Dev.* **1979**, *18*, 275–278.
- (44) Yu, X.-Y.; Bao, Z.-C.; Barker, J. R. Free Radical Reactions Involving Cl[·], Cl₂^{·−}, and SO₄^{2−} in the 248 nm Photolysis of Aqueous Solutions Containing S₂O₈^{2−} and Cl. *J. Phys. Chem. A* **2004**, *108*, 295–308.
- (45) Anipsitakis, G. P.; Dionysiou, D. D.; Gonzalez, M. A. Cobalt-Mediated Activation of Peroxymonosulfate and Sulfate Radical Attack on Phenolic Compounds. Implications of Chloride Ions. *Environ. Sci. Technol.* **2006**, *40*, 1000–1007.

Received for review March 13, 2010
 Revised manuscript received July 22, 2010
 Accepted July 28, 2010

IE100607U